

Synthesis, antifungal, antibacterial activity, and computational evaluations of some novel coumarin-1,2,4-triazole hybrid compounds

Karnaš, Maja; Rastija, Vesna; Vrandečić, Karolina; Ćosić, Jasenka; Kanižai Šarić, Gabriella; Agić, Dejan; subarić, Domagoj; Molnar, M.

Source / Izvornik: **JOURNAL OF TAIBAH UNIVERSITY FOR SCIENCE, 2024, 18, 1 - 16**

Journal article, Published version

Rad u časopisu, Objavljena verzija rada (izdavačev PDF)

<https://doi.org/10.1080/16583655.2024.2331456>

Permanent link / Trajna poveznica: <https://um.nsk.hr/um:nbn:hr:151:479195>

Rights / Prava: [In copyright](#)/[Zaštićeno autorskim pravom.](#)

Download date / Datum preuzimanja: **2024-07-01**



Sveučilište Josipa Jurja
Strossmayera u Osijeku

**Fakultet
agrobiotehničkih
znanosti Osijek**

Repository / Repozitorij:

[Repository of the Faculty of Agrobiotechnical
Sciences Osijek - Repository of the Faculty of
Agrobiotechnical Sciences Osijek](#)





Synthesis, antifungal, antibacterial activity, and computational evaluations of some novel coumarin-1,2,4-triazole hybrid compounds

Maja Karnaš, Vesna Rastija, Karolina Vrandečić, Jasenka Čosić, Gabriella Kanižai Šarić, Dejan Agić, Domagoj Šubarić & Maja Molnar

To cite this article: Maja Karnaš, Vesna Rastija, Karolina Vrandečić, Jasenka Čosić, Gabriella Kanižai Šarić, Dejan Agić, Domagoj Šubarić & Maja Molnar (2024) Synthesis, antifungal, antibacterial activity, and computational evaluations of some novel coumarin-1,2,4-triazole hybrid compounds, Journal of Taibah University for Science, 18:1, 2331456, DOI: [10.1080/16583655.2024.2331456](https://doi.org/10.1080/16583655.2024.2331456)

To link to this article: <https://doi.org/10.1080/16583655.2024.2331456>



© 2024 The Author(s). Published by Informa UK Limited, trading as Taylor & Francis Group.



[View supplementary material](#)



Published online: 27 Mar 2024.



[Submit your article to this journal](#)



Article views: 301



[View related articles](#)



[View Crossmark data](#)

Synthesis, antifungal, antibacterial activity, and computational evaluations of some novel coumarin-1,2,4-triazole hybrid compounds

Maja Karniša^a, Vesna Rastija^{ib}, Karolina Vrandečić^a, Jasenka Čosić^a, Gabriella Kanižai Šarić^a, Dejan Agić^a, Domagoj Šubarić^a and Maja Molnar^b

^aFaculty of Agrobiotechnical Sciences Osijek, Josip Juraj Strossmayer University of Osijek, Vladimira Preloga 1, Osijek HR-31000, Croatia;

^bFaculty of Food Technology Osijek, Josip Juraj Strossmayer University of Osijek, Franje Kuhača 18, Osijek HR-31000, Croatia

ABSTRACT

Effective plant pathogen control presents an important challenge. Pesticide resistance and associated health and environmental problems demonstrate the need for novel, safe active ingredients for plant protection. Since both coumarins and 1,2,4-triazoles show pesticidal activity, in this study, we evaluated the antimicrobial activity of coumarin-1,2,4-triazole hybrids against plant pathogenic fungi (*Fusarium oxysporum*, *Fusarium culmorum*, *Macrophomina phaseolina* and *Sclerotinia sclerotiorum*), bacterial plant pathogens (*Pseudomonas syringae* and *Rhodococcus fascians*), and beneficial bacteria (*Bacillus mycoides* and *Bradyrhizobium japonicum*). Coumarin-1,2,4-triazoles inhibited the growth of *S. sclerotiorum* and *F. oxysporum*, while no antibacterial effect on either pathogens or soil-beneficial bacteria was observed. A quantitative structure–activity relationship models for antifungal activities on *S. sclerotiorum* and *F. oxysporum*, developed using Dragon descriptors, can explain 79% and 77% of the compounds inhibitory activity, respectively. According to molecular docking, title compounds are potential sterol 14 α -demethylase inhibitors, with 7-((5-mercapto-4-(*p*-tolyl)-4*H*-1,2,4-triazol-3-yl)methoxy)-4-methyl-2*H*-chromen-2-one as the promising candidate for further research in plant protection.

ARTICLE HISTORY

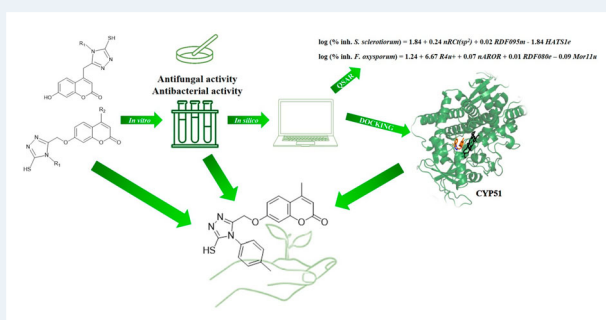
Received 28 December 2023

Revised 28 February 2024

Accepted 13 March 2024

KEYWORDS



Coumarin-1,2,4-triazoles; antimicrobial activity; QSAR; molecular docking; sterol 14 α -demethylase; plant protection




1. Introduction

Worldwide, plant pests and related diseases cause significant financial losses in agriculture [1]. *Fusarium* species are common fungal soil-borne pathogens damaging a variety of food and horticultural crops by causing rots, damping-off diseases, and vascular wilts. Several *Fusarium* species also have the ability to produce mycotoxins in food and agricultural products [2, 3]. Nine *Fusarium* species were identified in wheat plants in Croatia, of which *F. graminearum* and *F. culmorum* are more prominent eastern Croatia [4]. On the other hand, *F. oxysporum* f. sp. *lycopersici* is the main cause of tomato blight disease [2]. *Sclerotinia sclerotiorum* and *Macropomina phaseolina* are nonspecific, seed and soil-borne ascomycete fungi that infect more than 500 plant species, including oilseed crops, sugar beet, tobacco

and vegetables [5, 6]. *S. sclerotiorum* is considered a highly destructive plant pathogen causing severe crop damage and production loss [7]. The most common representatives of bacterial plant pathogens are *Pseudomonas syringae* and *Rhodococcus fascians*, both causing damage to economically important crop species [8, 9]. Thus, to ensure crop production, quality, and variety, it is necessary to control these pests. Most common fungicides, approved for use in the EU, for the treatment of aforementioned fungi are azole-based fungicides, such as metconazole, difenoconazole, and tebuconazole. It is estimated that approximately half of the total EU acreage under cereals and grapevine is treated with azole fungicides annually [10]. Their usage provided the advantage in plant protection, however, due to the increasing exposure many pathogens started

CONTACT Vesna Rastija  vesnakamencica@gmail.com  Faculty of Agrobiotechnical Sciences Osijek, Josip Juraj Strossmayer University of Osijek, Vladimira Preloga 1, Osijek HR-31000, Croatia

 Supplemental data for this article can be accessed online at <https://doi.org/10.1080/16583655.2024.2331456>.

© 2024 The Author(s). Published by Informa UK Limited, trading as Taylor & Francis Group.

This is an Open Access article distributed under the terms of the Creative Commons Attribution License (<http://creativecommons.org/licenses/by/4.0/>), which permits unrestricted use, distribution, and reproduction in any medium, provided the original work is properly cited. The terms on which this article has been published allow the posting of the Accepted Manuscript in a repository by the author(s) or with their consent.

to develop resistance [11–13]. Because of this, and the negative environmental effects some pesticides have shown [14, 15] there is an urgent need to find new, safer active ingredients.

Coumarins are a large group of natural and synthetic compounds. They can be found in nature in many plant families, but also as metabolites of various bacteria and fungi [16, 17]. In the biochemistry and physiology of plants, coumarins are known as compounds with antioxidant, antimicrobial, and insecticidal activity, inhibitors of various enzymes, but also as active participants in the regulation of plant growth and development, cellular respiration, and photosynthesis [18–28]. Triazoles are a group of heterocyclic compounds with three nitrogen atoms in a five-membered ring. All the atoms of the five-membered ring are sp^2 -hybridized, and 6 electrons are delocalized in π -molecular orbitals, increasing the aromatic stability of the system [29]. The structural motif of 1,2,4-triazole is found in compounds that exhibit antifungal, antioxidant, anti-inflammatory, antibacterial, antimycobacterial, antiviral, and antiparasitic effects [30–36]. 1,2,4-Triazoles are among the most common systemic fungicides used in the control of plant diseases. They are absorbed and transported in the plant, where they mostly hinder the growth and development of fungal mycelium [37]. The primary target for 1,2,4-triazole-based fungicides is the inhibition of the enzyme sterol 14α -demethylase. Its inhibition interferes with the biosynthesis of ergosterol, changing the fluidity of the membrane, leading to a decrease in the activity of key membrane-bound enzymes, and stopping the growth of fungal cells [38].

Hybrid compounds are extremely popular in medicinal chemistry due to exhibiting dual or multiple modes of action, which could also be applied to agrochemicals. Recently, we have employed a green method to synthesize hybrid compounds containing both coumarin and 1,2,4-triazole motifs [39], as their combination has been shown as efficacious in several instances [40–44]. Because of the potentially desirable pesticidal activity they might exhibit, in this study we tested their antimicrobial activity against phytopathogenic fungi and bacteria, to evaluate their potential as new active ingredients for plant protection products. Quantitative structure–activity relationship (QSAR) analysis was performed to find the relevant structural features responsible for the antifungal activity. For a better insight into a possible mechanism of action, a molecular docking study was performed on fungal lanosterol 14α -demethylase.

2. Experimental

2.1. General remarks

All chemicals and solvents were of analytical grade and purchased from commercial suppliers. Thin-layer

chromatography (TLC) was performed using fluorescent silica gel plates F254 (Merck, Darmstadt, Germany) and benzene : acetone : acetic acid (8 : 1 : 1 v/v) as an eluent. The melting point was determined on an electrothermal melting point apparatus (Electrothermal Engineering Ltd., Rochford, United Kingdom). ^1H and ^{13}C NMR spectra were recorded on a Bruker Avance 600 MHz NMR Spectrometer (Bruker Biospin GmbH, Rheinstetten, Germany) at 293 K with $\text{DMSO-}d_6$ as solvent and tetramethylsilane (TMS) as an internal standard. The mass spectra were recorded by LC/MS/MSAPI 2000 (Applied Biosystems/MDS SCIEX, CA, USA).

2.2. Synthesis procedure

The coumarin-1,2,4-triazoles used in this study were synthesized in a one-pot reaction between coumarin hydrazides and various isothiocyanates (ITC) in a deep eutectic solvent (DES) [39]. Briefly, coumarin hydrazides (1.0 eq, 1.6 mmol) and different ITCs (1.25 eq, 2.0 mmol) were added to the prepared choline chloride : urea (molar ratio 1 : 2) DES and stirred on a magnetic stirrer at 80 °C. The reaction progress was monitored by the TLC. After the completion of the reaction, the mixture was cooled to room temperature. Upon the addition of water, the crude product was collected by filtration and recrystallized in ethanol.

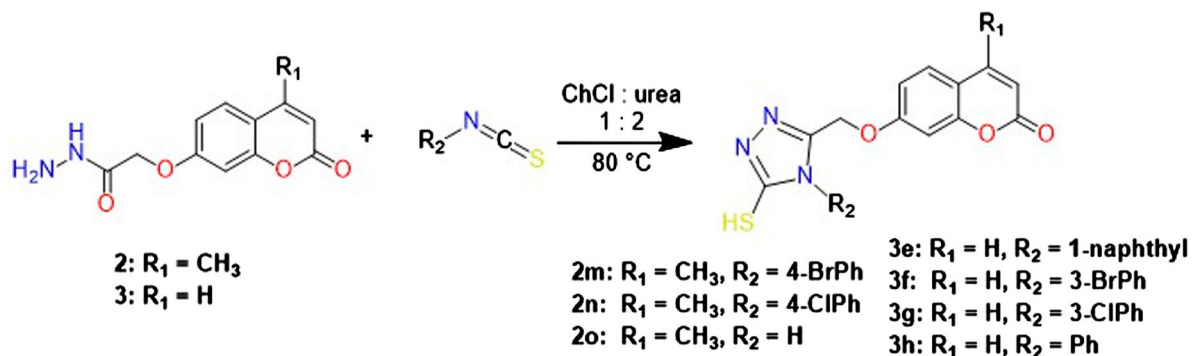
In addition to previously synthesized compounds (**1a** – **1k**, **2a** – **2l**, **3a** – **3d**) [39, 45], seven more were prepared using the described methodology; **2m** – **2o** from 2-((4-methyl-2-oxo-2H-chromen-7-yl)oxy)acetohydrazide (**2**), and **3e** – **3h** from 2-((2-oxo-2H-chromen-7-yl)oxy)acetohydrazide (**3**) (Scheme 1).

7-((4-(4-bromophenyl)-5-mercapto-4H-1,2,4-triazol-3-yl)methoxy)-4-methyl-2H-chromen-2-one(2m) [46]

$\text{C}_{19}\text{H}_{14}\text{BrN}_3\text{O}_3\text{S}$ Obtained in reaction of 0.397 g of compound **2** and 0.428 g of 4-bromophenyl ITC. White solid; Yield 39% (274 mg); $R_f = 0.62$; $mp = 216$ – 219 °C; MS: m/z 446.00 [M + H], $M_r = 444.30$; $^1\text{H-NMR}$ ($\text{DMSO-}d_6$, 300 MHz): δ /ppm 14.16 (1H, br. s, SH), 7.87 (1H, s, arom.), 7.61–7.75 (3H, m, arom.), 7.46 (1H, d, $J = 8.50$ Hz, arom.), 6.97–7.05 (2H, m, arom.), 6.23 (1H, s, C-3), 5.16 (2H, s, $-\text{CH}_2-$), 2.40 (3H, s, $-\text{CH}_3$); $^{13}\text{C-NMR}$ (CDCl_3 , 75 MHz): δ /ppm 168.6, 160.7, 160.1, 154.8, 153.3, 147.4, 130.3, 132.6, 132.3, 126.5, 122.9, 114.0, 112.5, 111.7, 101.9, 60.4, 18.1.

7-((4-(4-chlorophenyl)-5-mercapto-4H-1,2,4-triazol-3-yl)methoxy)-4-methyl-2H-chromen-2-one (2n) [46]

$\text{C}_{19}\text{H}_{14}\text{ClN}_3\text{O}_3\text{S}$ Obtained in reaction of 0.397 g of compound **2** and 0.339 g of 4-chlorophenyl ITC. White solid; Yield 83% (530 mg); $R_f = 0.61$; $mp = 208$ – 210 °C; MS: m/z 400.04 [M + H], $M_r = 399.85$; $^1\text{H-NMR}$ ($\text{DMSO-}d_6$, 300 MHz): δ /ppm 14.14 (1H, br. s, SH), 7.50–7.66



Scheme 1. Synthesis of compounds **2 m – 2o** and **3e – 3h**.

(5H, m, arom.), 6.97 (1H, d, $J = 2.37$ Hz, arom.), 6.85 (1H, dd, $J = 8.81, 2.37$ Hz, arom.), 6.24 (1H, s, C-3), 5.16 (2H, s, -CH₂-), 2.41 (3H, s, -CH₃); ¹³C-NMR (CDCl₃, 75 MHz): δ /ppm 168.7, 159.9, 159.8, 154.3, 153.2, 147.5, 129.3, 134.3, 132.1, 130.0, 126.5, 113.9, 112.3, 111.7, 101.9, 60.4, 18.1.

7-((5-mercapto-4H-1,2,4-triazol-3-yl)methoxy)-4-methyl-2H-chromen-2-one (2o)

C₁₃H₁₁N₃O₃S Obtained in reaction of 0.397 g of compound **2** and 0.194 g of potassium ITC. White solid; Yield 41% (191 mg); $R_f = 0.06$; $mp = 227$ – 230 °C; MS: m/z 292.16 [M + 2H], $M_r = 289.31$; ¹H-NMR (DMSO-*d*₆, 300 MHz): δ /ppm 9.86 (1H, s, NH), 7.70 (1H, d, $J = 8.80$ Hz, arom.), 7.03 (1H, dd, $J = 8.23, 1.41$ Hz, arom.), 6.98 (1H, d, $J = 2.34$ Hz, arom.), 6.22 (1H, s, C-3), 4.70 (2H, s, -CH₂-), 2.40 (3H, s, -CH₃); ¹³C-NMR (CDCl₃, 75 MHz): δ /ppm 166.9, 160.7, 160.0, 154.5, 153.3, 126.4, 113.5, 112.5, 111.4, 101.6, 66.2, 18.1.

7-((5-mercapto-4-(naphthalen-1-yl)-4H-1,2,4-triazol-3-yl)methoxy)-2H-chromen-2-one (3e)

C₂₂H₁₅N₃O₃S Obtained in reaction of 0.374 g of compound **3** and 0.370 mg of naphthyl ITC. White solid; Yield 84% (537 mg); $R_f = 0.61$; $mp = 231$ – 233 °C; MS: m/z 402.18 [M + H], $M_r = 401.44$; ¹H-NMR (DMSO-*d*₆, 300 MHz): δ /ppm 14.27 (1H, s, SH), 8.00–8.08 (2H, m, arom.), 7.87 (1H, d, $J = 9.52$ Hz, arom.), 7.54–7.63 (7H, m, arom.), 7.40 (1H, d, $J = 8.65$ Hz, arom.), 6.60 (1H, d, $J = 2.41$ Hz, arom.), 5.04 (2H, s, -CH₂-). ¹³C-NMR (CDCl₃, 75 MHz): δ /ppm 169.4, 160.0, 159.7, 154.7, 148.2, 144.0, 133.7–122.5, 113.1, 112.9, 112.1, 101.5, 60.5.

7-((4-(3-bromophenyl)-5-mercapto-4H-1,2,4-triazol-3-yl)methoxy)-2H-chromen-2-one (3f)

C₁₈H₁₂BrN₃O₃S Obtained in reaction of 0.374 g of compound **3** and 0.428 g of 3-bromophenyl ITC. Pale yellow solid; Yield 42% (287 mg); $R_f = 0.66$; $mp = 201$ – 203 °C; MS: m/z 431.52 [M + H], $M_r = 430.28$; ¹H-NMR (DMSO-*d*₆, 300 MHz): δ /ppm 14.14 (1H, br.s, -SH), 7.98 (1H, d, $J = 9.52$ Hz, arom.), 7.69 (2H, m, arom.), 7.46–7.51 (4H, m, arom.), 6.84 (1H, dd, $J = 8.62, 2.43$ Hz, arom.), 6.31 (1H, d, $J = 9.50$ Hz, arom.), 5.16 (2H, s, -CH₂-). ¹³C-NMR (CDCl₃, 75 MHz): δ /ppm 168.7, 160.0, 159.9,

154.9, 147.3, 144.1, 134.6, 132.5, 131.1, 129.4, 127.5, 121.4, 113.2, 112.6, 101.9, 60.5.

7-((4-(3-chlorophenyl)-5-mercapto-4H-1,2,4-triazol-3-yl)methoxy)-2H-chromen-2-one (3g)

C₁₈H₁₂ClN₃O₃S Obtained in reaction of 0.374 g of compound **3** and 0.263 mL of 3-chlorophenyl ITC. White solid; Yield 58% (360 mg); $R_f = 0.66$; $mp = 206$ – 208 °C; MS: m/z 386.11 [M + H], $M_r = 385.82$; ¹H-NMR (DMSO-*d*₆, 300 MHz): δ /ppm 7.99 (1H, d, $J = 9.52$ Hz, arom.), 7.65 (1H, m, arom.), 7.54–7.60 (3H, m, arom.), 7.48 (1H, m, arom.), 6.98 (1H, d, $J = 2.41$ Hz, arom.), 6.82 (1H, dd, $J = 8.62, 2.44$ Hz, arom.), 6.31 (1H, s, C-3), 5.16 (2H, s, -CH₂-); ¹³C-NMR (CDCl₃, 75 MHz): δ /ppm 168.7, 160.0, 159.9, 154.9, 147.4, 144.1, 134.5, 133.2, 130.8, 129.7, 128.3, 127.1, 113.2, 112.8, 112.6, 101.9, 60.5.

7-((5-mercapto-4-phenyl-4H-1,2,4-triazol-3-yl)methoxy)-2H-chromen-2-one(3h) [47]

C₁₈H₁₃N₃O₃S Obtained in reaction of 0.374 g of compound **3** and 0.239 mL of phenyl ITC. White solid; Yield 58% (326 mg); $R_f = 0.59$; $mp = 233$ – 234 °C; MS: m/z 352.15 [M + H], $M_r = 351.38$; ¹H-NMR (DMSO-*d*₆, 300 MHz): δ /ppm 7.97 (1H, m, arom.), 7.84–7.88 (2H, m, arom.), 7.43–7.67 (5H, m, arom.), 6.82 (1H, dd, $J = 8.61, 2.26$ Hz, arom.), 6.30 (1H, dd, $J = 9.45, 1.51$ Hz, arom.), 5.11 (2H, s, -CH₂-); ¹³C-NMR (CDCl₃, 75 MHz): δ /ppm 168.7, 160.8, 160.2, 155.1, 147.5, 144.2, 133.2, 129.5, 129.4, 129.4, 129.2, 128.0, 113.1, 112.8, 112.6, 101.9, 60.5.

2.3. Antifungal assay

For the preparation of 4 μ mol/mL stock solutions of title compounds, the appropriate mass of each compound was weighed and dissolved in a DMSO: water (1:1 v/v) mixture. A volume of 1 mL of the stock solution was added to 49 mL of potato dextrose agar (PDA). The concentration of the compound in the resulting mixture was 0.08 μ mol/mL, and the volume fraction of DMSO in the mixture was 1%. Untreated PDA was used as a negative control. Antifungal analysis was performed on four fungi (*Fusarium oxysporum* f. sp. *lycopersici*, *Fusarium culmorum*, *Macrophomina phaseolina*, and *Sclerotinia sclerotiorum*), all from the collection of

the Department of Phytopathology, Faculty of Agrobiotechnical Sciences Osijek. The assay was carried out following the method described in Siber et al [48]. Petri dishes were kept in a growth chamber at 22 ± 1 °C, with a 12 h light/12 h dark regime. The radial growth of the mycelium was measured 48 h after inoculation. Each measurement was performed in four replicates. The *in vitro* inhibiting effects of the compounds were expressed as the antifungal index (% growth inhibition). Commercially agricultural fungicides were used as a positive control at the concentration of 10 $\mu\text{g/mL}$, which corresponds to the molar concentration of the tested compounds. Strobilurin was used as a positive control for *F. culmorum*, *F. oxysporum*, and *S. sclerotiorum*, while mancozeb for *M. phaseolina* [49]. Mean values of % inhibition of the mycelial growth of tested compounds were compared with results of positive control by Fisher's test at $p \leq 0.05$ level with the aim of Statistica 14.1.0. (TIBCO, Santa Clara, CA, USA) [50].

2.4. Antibacterial assay

Stock solutions of compounds, 5.12 mg/mL, were prepared by dissolving 2.048 mg of each compound in 40 μL of DMSO and adding up to 400 μL of sterilized distilled water. Antibacterial activity was determined as the minimum inhibitory concentration (MIC) of the tested bacteria by the broth microdilution method [51]. The tested bacteria were two pathogenic bacteria *Pseudomonas syringae* DSM 50256 (Gram-negative) and *Rhodococcus fascians* DSM 20669 (Gram-positive), and two beneficial soil organisms, *Bacillus mycoides* from the collection of the Department of Microbiology, Faculty of Agrobiotechnical Sciences Osijek (Gram-positive), and *Bradhyrhizobium japonicum* DSM 1755 (Gram-negative). Bacterial cultures were multiplied on nutrient agar (Liofilchem, Italy) and Vincent agar. Stock solutions were diluted in the range from 512 to 1 $\mu\text{g/mL}$ in a sterile 96-well microtiter plate. Each well (except the control) contained 50 μL of broth with the compound of a certain concentration and was inoculated with 50 μL of pure bacterial cells at a density of 1.5×10^5 cells (CFU/mL). The plates were incubated at the optimal temperature and the results were checked after 48 h. The experiment was set up in four replicates, and the MIC was determined as the lowest compound concentration at which there was no visual turbidity of the nutrient medium.

2.5. QSAR analysis

Drawing and optimization of compound structures was performed in Avogadro 1.2.0. (University of Pittsburgh, Pittsburgh, PA, USA) [52]. Firstly, structures were optimized using the MM + molecular mechanics force field [53]. Afterward, the structures were subjected to geometry optimization using the AM1

semi-empirical method [54] with the Polak–Ribiere algorithm, until the root-mean-square gradient (RMS) was 0.1 kcal/(Åmol). Molecular descriptors were computed utilizing three-dimensional optimized structures of coumarin-1,2,4-triazoles using the Parameter Client (Virtual Computational Chemistry Laboratory), an electronic version of the Dragon software accessible at <https://vcclab.org/lab/pclient/> [55]. Antifungal activities of the tested compounds, expressed as % inhibition of mycelial growth of *S. sclerotiorum* and *F. oxysporum*, were converted into logarithmic values. Descriptors with more than 80% of constant values and values equal to zero, and inter-correlated descriptors ($R > 80\%$) were eliminated using QSARINS 2.2.4 (University of Insubria, Varese, Italy, 2019) [56]. For the external validation of the QSAR model, 20% of the compounds were chosen as the test set randomly. The best QSAR models were generated by genetic algorithm using QSARINS 2.2.4. The number of descriptors in the multiple regression equation was limited to three for *S. sclerotiorum*, and four for *F. oxysporum* [57]. The resulting QSAR models were evaluated using methods of internal and external validation. The Y-scrambling test was used to evaluate the model's robustness [58–60]. The applicability domain of the QSAR model was investigated by Williams plots (plotting residuals vs. leverage of compounds) [61].

2.6. Molecular docking analysis

To investigate the possible mode of antifungal activity for tested compounds, molecular docking was carried out using AutoDock Vina 1.1.2 software [62]. For this purpose, the crystal structure of lanosterol 14 α -demethylase from *Saccharomyces cerevisiae* with 1,2,4-triazole inhibitor difenoconazole, PDB ID: 5EAH [63] was extracted from the PDB. Before analysis, the co-crystallized ligand, difenoconazole (5LZ), was removed from the PDB file and saved for docking validation. MGL Tools 1.5.6 [64] was employed to prepare all structures for molecular docking. The docking site for the ligands on the enzyme was defined by a grid box with the dimensions $70 \times 70 \times 70$ Å, and center set at $x = 26.2$, $y = 12.4$, and $z = 18.4$. A docking simulation was performed with the standard 0.375 Å resolution. For each compound, 20 conformations were generated. Receptor–ligand interactions were visualized with BIOVIA Discovery Studio Visualizer 4.5 (Dassault Systèmes, San Diego, CA, USA) [65].

3. Results and discussion

3.1. Coumarin-1,2,4-triazoles synthesis

The synthetic strategy employed in our previous work [39] yielded seven more coumarin-1,2,4-triazole hybrids (Scheme 1). The compounds (**2m** – **2o**, **3e** – **3h**) were

obtained with satisfying yields (39–84%) and confirmed by spectral analyses (Supplementary Data). Structures of coumarin-1,2,4-triazoles synthesized in our previous work (**1a** – **1k**, **2a** – **2l**, **3a** – **3d**) are shown in Figure 1 [39, 45].

3.2. Biological activities

3.2.1. Coumarin-1,2,4-triazoles antifungal activity

Results of the coumarin-1,2,4-triazoles antifungal activity against phytopathogenic fungi at the 0.08 $\mu\text{mol/mL}$ concentration are given in Table 1. The percentages of growth inhibition were obtained by comparing the diameter of each treated fungal colony to the diameter of the negative control (untreated PDA). For all tested compounds, statistically significant lower inhibition was indicated regarding the inhibition of commercial agricultural fungicides.

Coumarin-1,2,4-triazoles effectively inhibited the mycelial growth of *S. sclerotiorum* and *F. oxysporum*. For *S. sclerotiorum* the growth percentage inhibition ranged from 26.51% (**3d**) to 76.06% (**2j**). Comparing the three series of compounds, the second series (triazole ring at C7 and a methyl group at C4 of coumarin) provided the strongest inhibitors of this pathogen. Compound **2j**, with a *p*-tolyl group on the triazole ring, showed the highest inhibition. Replacing that group with a benzyl group (**2c**) slightly reduced the efficiency, while the 3-bromophenyl (**2f**), phenyl (**2l**), 3-chlorophenyl (**2e**) and ethyl (**2k**) derivatives were weaker by only 5–6%. In the first series of coumarin-1,2,4-triazoles there is one compound with high inhibition, **1g** with a 4-bromophenyl substituent on the triazole ring (74%). Replacing that substituent with benzyl (**1c**) or 3-methoxyphenyl (**1d**) group lowers the inhibitory potential by 10%. Compounds from the third series exhibited the lowest inhibition results. As this series differs from the second only by the lack of a methyl group at C4 of the coumarin nucleus, it is likely that its presence positively affects the ability to inhibit *S. sclerotiorum*.

All compounds exhibited an inhibitory effect on *F. oxysporum* as well, ranging from 35.09% (**1c**) to 74.09% (**2j**). Only one compound from the first series, with an ethyl substituent, surpasses 50% inhibition (**1j**, 57.51%). When substituted with a 4-chlorophenyl substituent (**1f**), the inhibition percentage decreased by up to 10%. In the second series of compounds, substitution of *p*-tolyl with 4-bromophenyl or naphthyl group led to a decrease in potency from 74.09% for **2j** to 54.59% and 53.62% for **2m** and **2h**, respectively. Compounds **2a** (40.94%), **2b** (41.92%), and **2o** (43.65%) with small substituents on the triazole ring showed the lowest inhibition. The third series of compounds showed similar inhibitory results as the second, and both were more potent against *F. oxysporum* when compared to the first. Thus, the position of the triazole ring at C7 of the

coumarin is again more favorable for the antifungal activity.

Coumarin-1,2,4-triazoles showed a much lower effect on *M. phaseolina* and *F. culmorum*. Compound **2j** showed the highest inhibition of *M. phaseolina* (35.38%). Three derivatives (**1j**, **2e**, and **2h**) exhibited no effect on *M. phaseolina* mycelium growth. For *F. culmorum*, the highest percentage of growth inhibition was determined for compound **2m** (31.25%). Thirteen derivatives, seven from the third series of compounds, did not show any influence on the growth of *F. culmorum* mycelia. By comparing the results between compounds, it is clear that the removal of the methyl group at C4 of the coumarin leads to the absence of activity on *F. culmorum*.

In general, the second series of coumarin-1,2,4-triazoles is more effective in antifungal activity compared to the first and third series, which indicates that such a structural arrangement is more favourable for this activity. Compound **2j** exhibited the highest results of mycelial growth inhibition in three of the four tested fungi. However, it is less efficient against *Fusarium* species than some commercial triazole fungicides at the same concentrations [66].

3.2.2. Antibacterial activity

The antibacterial effect of coumarin-1,2,4-triazoles was first tested on phytopathogenic bacteria, *Pseudomonas syringae* and *Rhodococcus fascians*. Results showed that none of the coumarin-1,2,4-triazoles had any effect on the tested pathogenic bacteria, even at the highest concentration of 512 $\mu\text{g/mL}$. Since the soil-beneficial bacteria can come into contact with applied pesticides as well, the influence of title compounds on two representatives of soil-beneficial bacteria, *Bacillus mycoides* [67] and *Bradhyrhizobium japonicum* [68] was tested. As with pathogenic bacteria, none of the coumarin-1,2,4-triazoles showed activity against the tested bacteria.

3.3. QSAR models for antifungal activity

3.3.1. QSAR model for *Sclerotinia sclerotiorum*

The best QSAR model for antifungal activity against *S. sclerotiorum* is:

$$\begin{aligned} \log (\% \text{ inh. } S. \text{ sclerotiorum}) &= 1.84 + 0.24nRcT(sp^2) + 0.02RDF095m \\ &\quad - 1.84HATS1e \end{aligned} \quad (1)$$

where $nRcT(sp^2)$ is the number of aliphatic tertiary carbon atoms (sp^2), $RDF095m$ is the mass-weighted radial distribution function at 9.5 Å, and $HATS1e$ is the Sander-son electronegativity-weighted 3D-autocorrelation descriptor. The test set for the external validation contained 6 randomly selected compounds. Variables in

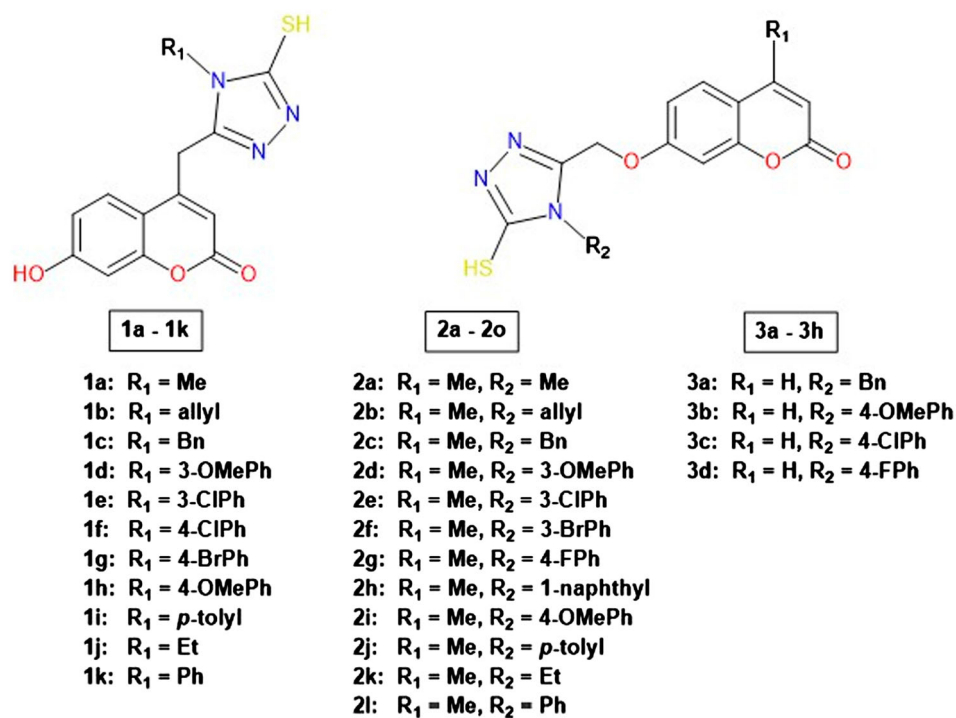


Figure 1. General structures of previously synthesized coumarin-1,2,4-triazoles.

the model equation are ranked by relative importance according to their standardized regression coefficient. The most important statistical parameters of the selected model are given in Table 2. The collinearity of the descriptors in the model was assessed using the correlation matrix (Supplementary Data T1), and the possibility of overfitting was ruled out (correlation coefficients are less than 0.7). The values of multivariate correlation index (K_{xx}) and global correlation among descriptors (ΔK) additionally confirm that a linear relationship among descriptors does not exist. According to the coefficient of determination (R^2), this model can explain 79% of the inhibitory effect of coumarin-1,2,4-triazoles on *S. sclerotiorum*. The stability and robustness of the model were confirmed by cross-validation by the leave-one-out (LOO) and the leave-many-out (LMO) procedures. The cross-validated explained variances, (Q^2_{LOO} and Q^2_{LMO}) are higher than 0.6. Also, the values of both coefficients obtained by the Y-scramble method, correlation coefficient (R^2_{Yscr}), and cross-validation coefficient (Q^2_{Yscr}) have values < 0.02 , showing that the model was not developed by chance [58, 69]. External validation confirmed the predictive ability of this model: R^2_{ext} is > 0.60 ; the concordance correlation coefficient of the test set (CCC_{ext}) is > 0.80 ; root-mean-square error ($RMSE_{ex}$) and mean absolute error (MAE_{ex}) are close to zero, as well as predictive squared correlation coefficients (Q^2_{Fn}) are higher than 0.60 [59, 70].

The applicability domain inspected by the Williams diagram (Figure 2) revealed no compound is outside the warning leverage ($h^* = 0.429$). Compound **1f**, whose cross-validated standardized residual is greater than two standard deviation units, was identified as an

outlier [61]. However, its exclusion did not improve the quality of the model. The values of experimental and calculated by model activities, as well as the values of descriptors in the model equation for each compound are given in Supplementary Data T3.

The first independent variable in the model (1) is the number of aliphatic tertiary carbon atoms in the compound [71]. The positive regression coefficient of this descriptor in the model equation indicates the importance of the presence of sp^2 tertiary aliphatic carbon atom within the structure of the compound. Such an atom is presented in both the first and second series of coumarin-1,2,4-triazoles, while it is absent in the third, where weak inhibition results were observed. Its presence, therefore, has a positive effect on antifungal activity. The second variable in the QSAR model is the radial distribution function (RDF) descriptor. The RDF of a set of atoms can be interpreted as the probability of finding atoms in a spherical volume of a given radius [71]. Descriptor $RDF095m$ contains information on the three-dimensional distribution of mass in molecules within a radius of 9.5 Å from the geometric center of the molecule. The compounds with the largest molecular radius and molecular mass also have the largest values of this descriptor. Its positive regression coefficient in the model indicates that for better antifungal activity against *S. sclerotiorum*, coumarin-1,2,4-triazoles should have heavier atoms distributed on the border of the mentioned radius. The last variable in the model is $HATS1e$, a GETAWAY (GEometry, Topology, and AtomWeights Assembly) descriptor. $HATS$ (H -matrix derived Autocorrelation of a Topological Structure) descriptors coordinate 3D molecular geometry

Table 1. Percentage inhibition (%) of the mycelial growth of phytopathogenic fungi 48 h after inoculation with coumarin-1,2,4-triazoles at 0.08 $\mu\text{mol/mL}$ concentration (results are expressed as the mean of four replicates \pm standard deviation).

Comp.	<i>S. sclerotiorum</i>	<i>M. phaseolina</i>	<i>F. oxysporum</i>	<i>F. culmorum</i>
1a	37.26 \pm 4.76	3.82 \pm 3.15	43.86 \pm 4.73	n.a.
1b	40.34 \pm 4.14	26.78 \pm 2.73	44.83 \pm 4.39	n.a.
1c	64.92 \pm 2.24	10.51 \pm 2.62	35.09 \pm 4.95	11.60 \pm 2.10
1d	63.39 \pm 5.14	19.12 \pm 2.23	39.97 \pm 2.89	11.60 \pm 2.10
1e	58.77 \pm 5.58	30.60 \pm 2.23	37.04 \pm 2.96	16.97 \pm 4.21
1f	35.35 \pm 0.97	21.99 \pm 3.44	47.75 \pm 3.44	n.a.
1g	74.14 \pm 2.44	23.91 \pm 4.17	39.97 \pm 4.73	14.28 \pm 2.10
1h	54.94 \pm 3.78	3.82 \pm 2.73	45.82 \pm 3.44	n.a.
1i	47.86 \pm 2.56	23.91 \pm 3.69	39.81 \pm 4.00	10.42 \pm 2.85
1j	35.35 \pm 0.00	n.a.	57.51 \pm 8.11	n.a.
1k	46.10 \pm 8.25	21.04 \pm 5.69	38.01 \pm 3.92	14.28 \pm 4.21
2a	65.31 \pm 2.05	15.30 \pm 3.86	40.94 \pm 5.46	4.46 \pm 2.10
2b	66.46 \pm 7.18	8.61 \pm 3.86	41.92 \pm 5.42	25.00 \pm 4.21
2c	74.91 \pm 4.21	21.03 \pm 1.58	48.74 \pm 2.96	25.00 \pm 3.44
2d	62.23 \pm 6.14	1.92 \pm 0.86	47.75 \pm 5.09	n.a.
2e	69.54 \pm 4.57	n.a.	45.82 \pm 5.09	11.60 \pm 2.10
2f	71.07 \pm 3.91	16.25 \pm 1.93	48.74 \pm 3.97	12.50 \pm 2.98
2g	68.38 \pm 4.48	24.86 \pm 6.50	47.75 \pm 3.92	20.53 \pm 4.20
2h	62.62 \pm 4.25	n.a.	53.62 \pm 5.09	8.93 \pm 1.73
2i	57.24 \pm 12.71	20.08 \pm 1.58	49.71 \pm 4.34	28.57 \pm 4.21
2j	76.06 \pm 4.37	35.38 \pm 2.62	74.09 \pm 3.24	28.57 \pm 2.98
2k	69.54 \pm 2.44	9.56 \pm 4.17	46.78 \pm 4.95	1.79 \pm 1.48
2l	71.46 \pm 4.37	2.87 \pm 1.58	49.71 \pm 2.20	9.82 \pm 1.72
2m	68.77 \pm 3.11	6.69 \pm 2.73	54.59 \pm 1.87	31.25 \pm 2.10
2n	67.99 \pm 4.46	10.51 \pm 2.74	48.74 \pm 6.07	12.50 \pm 1.72
2o	57.54 \pm 3.84	21.04 \pm 3.44	43.65 \pm 3.44	10.72 \pm 3.84
3a	33.03 \pm 3.41	4.79 \pm 2.73	52.63 \pm 6.88	n.a.
3b	44.17 \pm 1.14	12.43 \pm 2.62	46.78 \pm 5.30	7.14 \pm 2.80
3c	40.34 \pm 3.26	16.25 \pm 1.93	47.75 \pm 3.44	n.a.
3d	26.51 \pm 3.40	21.04 \pm 3.53	49.71 \pm 2.20	n.a.
3e	30.90 \pm 3.91	23.90 \pm 3.35	51.29 \pm 4.02	n.a.
3f	42.66 \pm 3.75	8.62 \pm 2.64	44.67 \pm 4.49	n.a.
3g	37.15 \pm 4.37	3.82 \pm 2.33	45.71 \pm 3.69	n.a.
3h	37.15 \pm 2.23	15.30 \pm 4.46	51.28 \pm 2.29	n.a.
Negative control	0.00 \pm 0.00	0.00 \pm 0.00	0.00 \pm 0.00	0.00 \pm 0.00
Positive control*	93.20 \pm 0.00 strobilurin	88.10 \pm 0.00 mancozeb	82.50 \pm 0.00 strobilurin	87.50 \pm 0.00 strobilurin

n.a. – no effect on mycelial growth; *Commercially agricultural fungicide at a concentration 10 $\mu\text{g/mL}$.

and interatomic bonds via a molecular influence matrix. These H-GETAWAY descriptors are calculated from the leverage matrix obtained from the centered atomic coordinates or molecular influence matrix (H). Values of $HATS1e$ depend on interactions between two electronegative atoms (O, N, S, and halogens) distributed closely in the three-dimensional optimized structure of a molecule [72]. The negative coefficient in Eq. 1 implies that compounds with enhanced values of $HATS1e$ have improved antifungal activity. A graphical representation of important structural features revealed by the QSAR models is presented in Scheme 2.

3.3.2. QSAR model for *Fusarium oxysporum*

The best QSAR model for antifungal activity against *F. oxysporum* is:

$$\begin{aligned} \log (\% \text{inh. } F. \text{oxysporum}) \\ = 1.24 + 6.67R4u + +0.07nAROR + 0.01RDF080e \\ - 0.09Mor11u \end{aligned} \quad (2)$$

where $R4u+$ represents the R maximum autocorrelation at topological distance 4 (unweighted), $nAROR$ the number of aromatic ether groups, $RDF080e$ the

radial distribution function at 8 Å weighted by Sander-son electronegativity, and $Mor11u$ the unweighted 3D-MoRSE descriptor. The test set for the external validation contained 6 randomly selected compounds. Variables in the model equation are ordered by relative importance according to their standardized regression coefficient. The collinearity of the descriptors in the model was assessed using the correlation matrix and no correlation between the descriptors in the model was observed (Supplementary Data T2).

The most important statistical parameters for the selected QSAR model all satisfy the criteria (Table 2). According to the R^2 , the model can explain 77% of the inhibitory effect of the compounds on *F. oxysporum*. The stability and robustness of this model were confirmed by the internal validation coefficients Q^2_{LOO} and Q^2_{LMO} , both higher than 0.6. Satisfactory values of the R^2_{Yscr} and Q^2_{Yscr} coefficients were obtained as well [58, 69]. The predictive ability of the model was confirmed by high R^2_{ext} , small differences between $RMSE$ of the training set and $RMSE_{ext}$, as well as between MAE of the training set and MAE_{ext} [59, 70].

Inspection of the Williams plot (Figure 3) for the applicability domain of model (2) revealed one outlier (1j). The most active compound 2j, slightly exceeds the warning value ($h^* = 0.536$), therefore its predicted

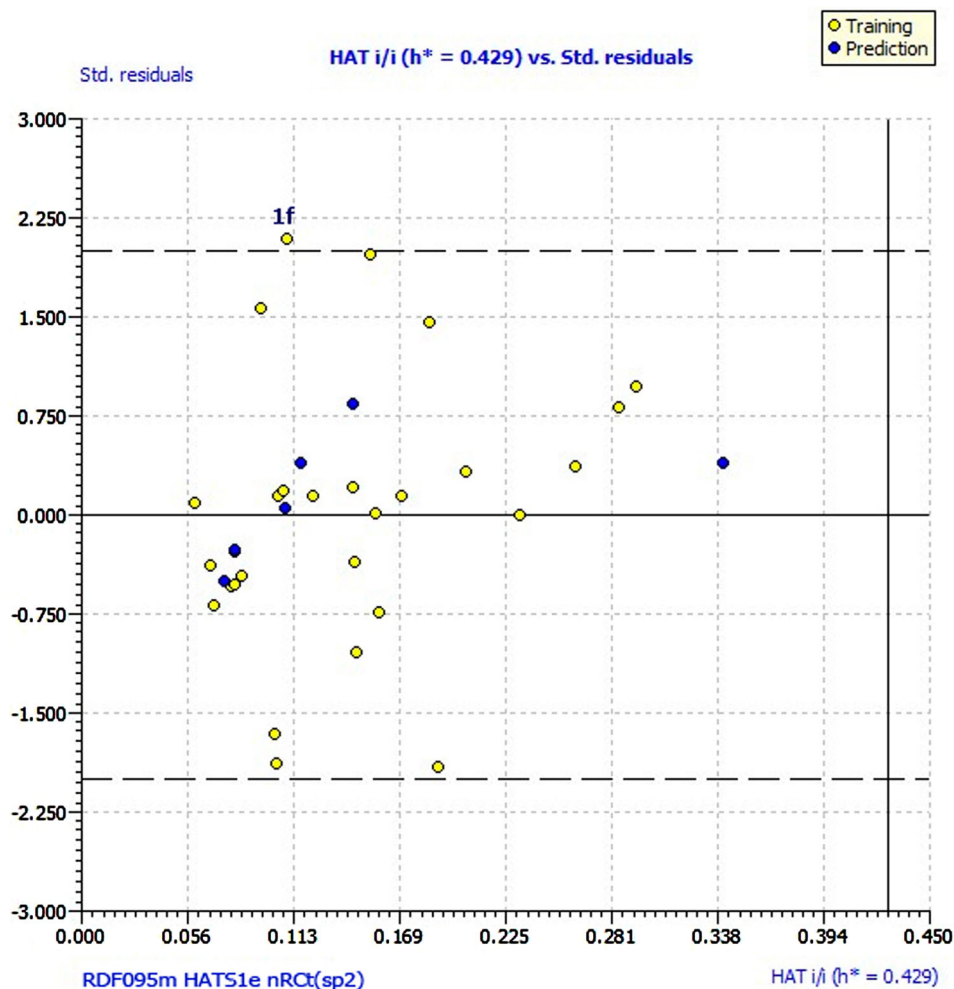
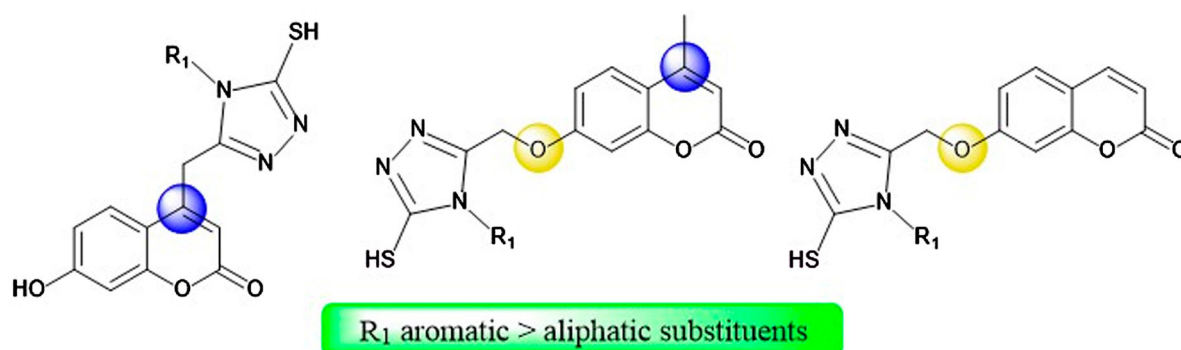


Figure 2. Williams plot of applicability domain of the QSAR model (1) for the inhibition of *Sclerotinia sclerotiorum*.



Scheme 2. Graphical representation of important structural features revealed by QSAR models (blue for model (1), yellow for model (2), and green for both models).

value is not reliable [61]. The values of experimental and calculated by model activities, as well as the values of descriptors in the model equation for each compound are given in Supplementary Data T4.

The first variable in the model equation is the 3D-GETAWAY descriptor $R4u+$. It belongs to the R-GETAWAY descriptors that combine the information obtained from the molecular influence matrix with the interatomic distances in the molecule. The descriptor $R4u+$ is derived from the influence/distance matrix, and, being unweighted, treats atoms equally at the

topological distance 4 [72]. A positive regression coefficient in the equation implies that higher values of this descriptor imply pronounced antifungal activity against *F. oxysporum*. Compounds with a larger number of terminal atoms arranged at a topological distance of 4 have higher $R4u+$ descriptor values and are more effective against *F. oxysporum*. The second variable is the number of aromatic ether groups in the structure of the compound [71]. A positive regression coefficient indicates the importance of this structural fragment for improved antifungal activity against *F. oxysporum*.

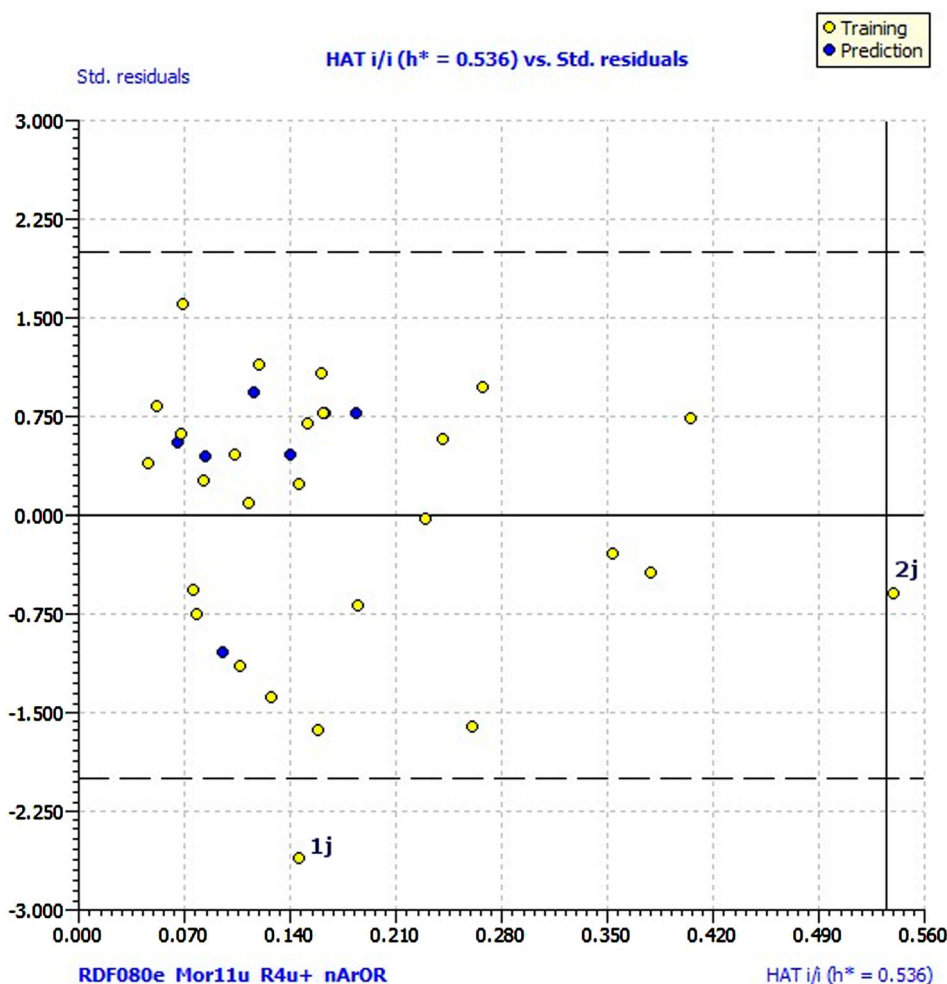


Figure 3. Williams plot of applicability domain of the QSAR model (2) for the inhibition of *Fusarium oxysporum*.

This descriptor is probably also the reason why compound **1j** is an outlier because it does not have an ether group, but shows high activity. The third variable in the model equation is the RDF descriptor [71]. The positive regression coefficient of the descriptor *RDF080e* suggests the occurrence of a linear dependence between the antifungal activity and the increased 3D distribution of atomic electronegativity within 8 Å of the geometric center of the molecule. The last variable, *Mor11u*, indicates the importance of the three-dimensional arrangement of all atoms in the molecule. *Mor11u* has a scattering parameter $s = 10 \text{ \AA}^{-1}$, and since it is not weighted, it treats all atoms equally [73]. Its negative coefficient in Equation 2 indicates that higher values of this descriptor would generally adversely affect the antifungal activity of coumarin-1,2,4-triazoles.

3.4. Molecular docking on lanosterol 14 α -demethylase

The enzyme lanosterol 14 α -demethylase (LDM, EC: 1.14.14.154) is a major target for azoles used in agriculture [37]. One of the nitrogen atoms in the azole ring coordinates as the sixth axial iron ligand in the

heme cofactor, blocking oxygen activation. LDM contains a relatively rigid ligand-binding pocket, with a deeply buried active site in which heme is located. Conserved residues in fungal demethylases are classified into three motifs and six putative substrate recognition sites (SRS). Among the three motifs, the most conserved are FXXGXXCXG, the heme-binding domain, and the E-R-R triad formed from the EXXR and PER motifs, which contribute to the heme stabilization. Of the six putative SRSs, SRS1 and SRS4 have been most thoroughly studied [74]. Regarding the *S. cerevisiae* LDM used for molecular docking analysis, heme binding domain consists of residues Phe463 – Gly472, and heme stabilization motifs are residues Glu372 – Arg375 and Ile428 – Arg430. SRS1 consists of Ala125 – Asn144 while SRS4 consists of Val311 – Trp325.

The molecular docking showed that coumarin-1,2,4-triazoles can all fit into the LDM active site, with binding energy values from -7.9 kcal/mol to -10.7 kcal/mol . More than half of the compounds show binding affinity equal to or greater than difenoconazole (-10.0 kcal/mol). Among them, most belong to the second series of coumarin-1,2,4-triazoles, which coincides with the experimentally obtained data of antifungal activity on all four fungi. To validate the analysis, re-docking

Table 2. The statistical results of QSAR models for antifungal activity

Statistical parameters	Model (1) for <i>S. sclerotiorum</i>	Model (2) for <i>F. oxysporum</i>
$N_{\text{trainingset}}$	28	28
N_{testset}	6 (1a, 1h, 2h, 2l, 2o, 3a)	6 (1d, 1i, 2f, 2g, 2m, 2o)
R^2	0.79	0.77
R^2_{adj}	0.76	0.74
s	0.07	0.03
F	29.75	19.74
K_{xx}	0.23	0.22
ΔK	0.15	0.05
$RMSE$	0.06	0.03
MAE	0.05	0.02
CCC	0.88	0.87
Q^2_{LOO}	0.71	0.68
Q^2_{LMO}	0.69	0.63
$RMSE_{cv}$	0.07	0.04
MAE_{cv}	0.05	0.03
CCC_{cv}	0.84	0.82
R^2_{Yscr}	0.11	0.15
Q^2_{Yscr}	-0.22	-0.29
R^2_{ext}	0.97	0.88
CCC_{ext}	0.97	0.88
$RMSE_{\text{ext}}$	0.03	0.02
MAE_{ext}	0.03	0.02
Q^2_{F1}	0.94	0.81
Q^2_{F2}	0.94	0.80
Q^2_{F3}	0.95	0.87
$r^2_m \text{ aver}$	0.81	0.62
$r^2_m \text{ diff}$	0.06	0.18

R^2 (coefficient of determination); R^2_{adj} (adjusted coefficient of determination); s (standard deviation of regression); F (Fisher ratio); K_{xx} (multivariate correlation index); ΔK (global correlation among descriptors); $RMSE$ (root-mean-square error of the training set); MAE (mean absolute error of the training set); CCC (concordance correlation coefficient of the training set); Q^2_{LOO} (the leave-one-out cross-validated explained variance); Q^2_{LMO} (the leave-many-out cross-validated explained variance); $RMSE_{cv}$ (root-mean-square error of the training set determined through the cross validated method); MAE_{cv} (mean absolute error of the internal validation set); CCC_{cv} (concordance correlation coefficient test set using cross validation); R^2_{Yscr} (Y-scramble correlation coefficients); Q^2_{Yscr} (Y-scramble cross-validation coefficients); $RMSE_{\text{ext}}$ (root-mean-square error of the external validation set); MAE_{ext} (mean absolute error of the external validation set); R^2_{ext} (coefficient of determination of validation set); Q^2_{Fn} (predictive squared correlation coefficients); CCC_{ext} (concordance correlation coefficient of the test set); $r^2_m \text{ average}$ (average value of squared correlation coefficients between the observed and (leave-one-out) predicted values of the compounds with and without intercept); $r^2_m \text{ difference}$ (absolute difference between the observed and leave-one-out predicted values of the compounds with and without intercept).

of co-crystallized difenoconazole was performed and compared to its original position. The root-mean-square deviation, $RMSD$, between the equivalent atoms of the co-crystallized and re-incorporated inhibitor was 0.565 Å, which satisfied the standard validation conditions [75, 76]. Figure 4 shows the binding site of LDM with difenoconazole. The triazole ring together with the cysteine from the heme-binding domain (Cys470) coordinate the iron ion [38, 62]. The distance between triazole ring π -orbitals and Cys470 sulphur is 5.65 Å. Four close π -interactions (3.34–5.26 Å) with heme are present (π -sigma, π -alkyl, and π - π T-shaped interactions between difenoconazole phenyl rings and heme pyrrole rings, and one alkyl interaction with the far most chlorine substituent). Difenoconazole also interacts with residues from SRS1 (π -sigma interactions with Tyr126, and alkyl/ π -alkyl interactions with Phe134 and

Ile139) and SRS4 (π -sigma interaction with Thr318) (Figure 4 and Supplementary Data T5).

The best orientation of the experimentally strongest compound **2j** shows it positioned itself parallel to the heme. The coumarin motif is closer to the heme, while the terminal p -tolyl substituent is rotated so that it is parallel to both the coumarin core and the heme. The binding energy of compound **2j** to LDM is -10.0 kcal/mol, the same as the co-crystallized difenoconazole. Figure 5 shows the binding site of compound **2j**, where it is visible how the coumarin nucleus, more precisely the benzene ring, coordinates with the iron. The analysis of the most important interactions of compound **2j** with LDM residues showed it is an π -cation interaction between the benzene ring of coumarin and the iron ion. Compound **2j** additionally creates two hydrogen bonds with residues from SRS4: N1 of the triazole ring with Tyr126 (3.03 Å) and O of the pyrone ring with Tyr140 (2.09 Å). The π -sigma interaction between the triazole ring and Leu380 (3.84 Å), and the π - π T-shaped interaction (5.18 Å, with a dihedral angle of 89.869°) between the p -tolyl substituent and Phe236 also contribute to the stabilization of compound **2j**. The remaining interactions are predominantly with residues from the SRS1 and SRS4 subunits (Figure 5 and Supplementary Data T5).

The highest binding energy was obtained for compound **2e** (-10.7 kcal/mol). Its best orientation in the LDM binding site is very similar to that of compound **2j**. The analysis of the most important interactions shows that compound **2e** has the same types of interactions with the same residues as compound **2j** (Supplementary Data T5). Two hydrogen bonds are between the same atoms at similar distances (3.04 Å with Tyr126 and 2.26 Å with Tyr140). The only difference, and consequently the reason for the slightly better binding energy of compound **2e**, is the interaction between the chlorine atom of the terminal chlorophenyl substituent of **2e** and glycine (Gly314) which is part of the SRS4 subunit (Figure 6).

4. Conclusion

Coumarin-1,2,4-triazole hybrids effectively inhibited the mycelial growth of plant pathogenic fungi *S. sclerotiorum* and *F. oxysporum*, however showed no effect on bacteria. Compounds with a triazole ring at C7 and a methyl group at C4 of coumarin core had stronger antifungal activity compared to the others, indicating that such structural arrangement is more favourable. QSAR models indicated that for enhanced antifungal activity the compounds need a longer linker between triazole and coumarin motifs, an additional tertiary sp^2 carbon atom or ether group, and electronegative substituents for improved distribution of atoms within the radii indicated by the descriptors. Molecular docking showed that all compounds fit well into the fungal lanosterol

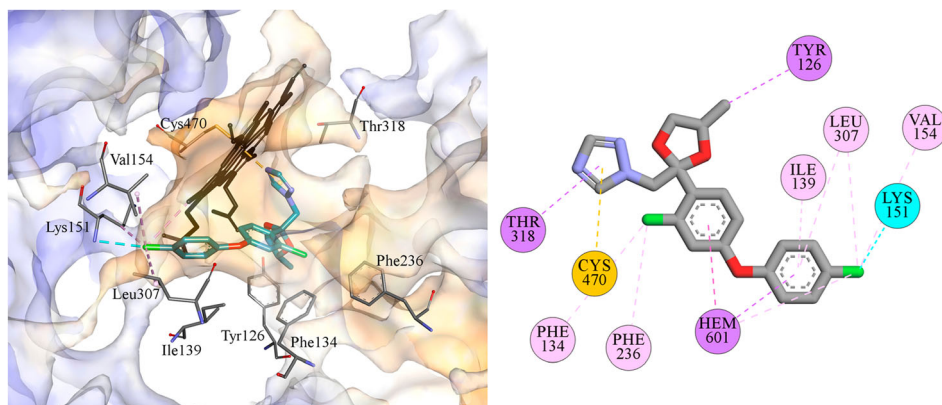


Figure 4. Co-crystallized difenoconazole in the LDM binding site. **Left:** 3D representation of the hydrophobic surface of the enzyme (increase in hydrophobicity from blue to orange) with highlighted heme (black sticks) and amino acids (grey sticks) interacting with difenoconazole (blue sticks). **Right:** 2D representation of difenoconazole and LDM interactions (orange – π -sulfur; blue – halogen; pink – π -sigma; pink – alkyl and π -alkyl interactions).

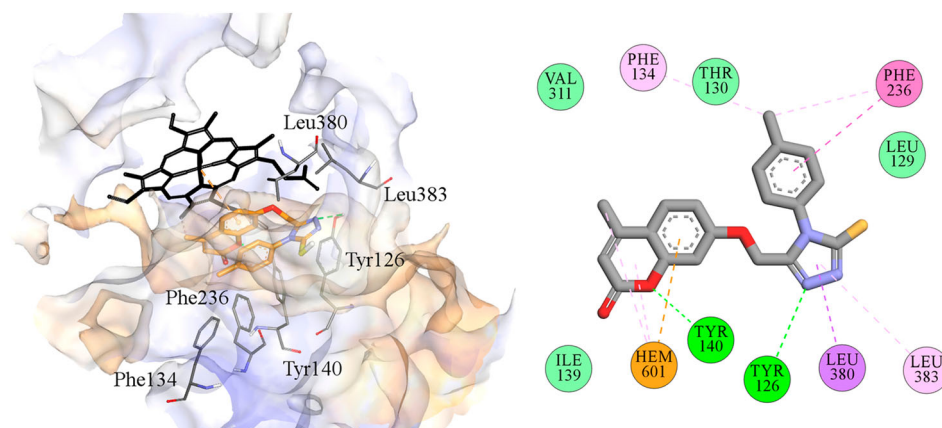


Figure 5. Compound **2j** in the LDM binding site. **Left:** 3D representation of the hydrophobic surface of the enzyme (increasing hydrophobicity from blue to orange) with highlighted heme (black sticks) and the most important amino acids (grey sticks) interacting with **2j** (orange sticks). **Right:** 2D representation of the interactions of **2j** and LDM (green – hydrogen bond; light green – van der Waals; orange – π -cation; purple – π -sigma; pink – π - π ; light pink – alkyl and π -alkyl interactions).

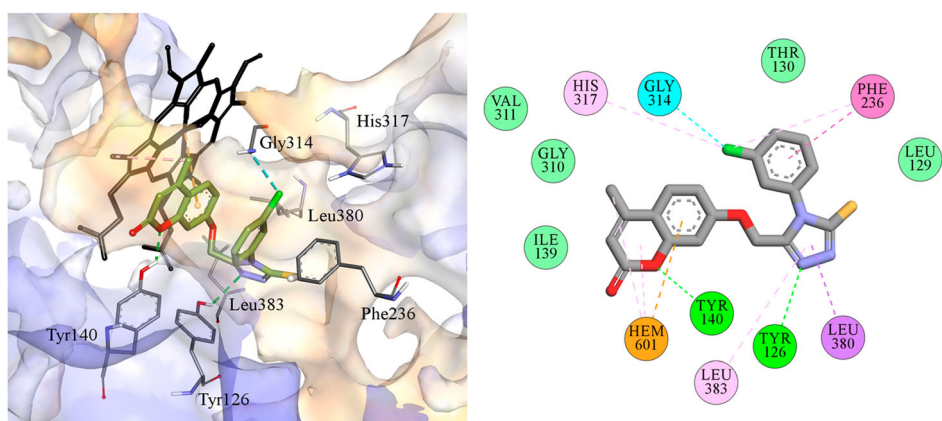


Figure 6. Compound **2e** in the LDM binding site. **Left:** 3D representation of the hydrophobic surface of the enzyme (increasing hydrophobicity from blue to orange) with highlighted heme (black sticks) and the most important amino acids (grey sticks) interacting with **2e** (gold sticks). **Right:** 2D representation of **2e** and LDM interactions (green – hydrogen bond; light green – van der Waals; blue – halogen; orange – π -cation; purple – π -sigma; pink – π - π ; light pink – alkyl and π -alkyl interactions).

14 α -demethylase active site, interacting with iron from heme cofactor. The most notable experimentally and computationally was compound **2j**, however further research is necessary to show if it could be a good candidate for a new eco-friendly, plant-protection active ingredient.

Acknowledgements

The synthesized compounds are an output from the research project of Croatian Science Foundation, “Green Technologies in Synthesis of Heterocyclic Compounds” (UIP-2017-05-6593).

Disclosure statement

No potential conflict of interest was reported by the author(s).

Funding

This work was supported by the Faculty of Agrobiotechnical Sciences Osijek, University of Osijek, under the project “DEFACTOPlant”, as part of the research team “Design of bioactive molecules”.

Availability of data and materials

All relevant data are within the manuscript and available from the corresponding author upon request.

ORCID

Vesna Rastija  <http://orcid.org/0000-0001-9542-4022>

References

- [1] Gavrilescu M, Pogăcean MO. Plant protection products and their sustainable and environmentally friendly use. *Environ Eng Manag J*. 2009;8:607–627. doi: 10.30638/eemj.2009.084
- [2] Srinivas C, Nirmala Devi D, Narasimha Murthy K, et al. *Fusarium oxysporum* f. sp. *lycopersici* causal agent of vascular wilt disease of tomato: biology to diversity—A review. *Saudi J Biol Sci*. 2019;26(7):1315–1324. doi: 10.1016/j.sjbs.2019.06.002
- [3] Scherm B, Balmas V, Spanu F, et al. The wheat pathogen *Fusarium culmorum*. *Mol Plant Pathol*. 2013;14:323–341. doi: 10.1111/mpp.12011
- [4] Čosić J, Vrandečić K, Šimić B, et al. *Fusarium* species isolated from plant debris in Eastern Croatia. *Cereal Res Commun*. 2008;36:55–58.
- [5] Hossain MM, Sultana F, Li W, et al. *Sclerotinia sclerotiorum* (Lib.) de bary: insights into the pathogenomic features of a global pathogen. *Cells*. 2023;12:1063. doi: 10.3390/cells12071063
- [6] Marquez N, Giachero ML, Declerck S, et al. *Macrophomina phaseolina*: general characteristics of pathogenicity and methods of control. *Front Plant Sci*. 2021;12:634397. doi: 10.3389/fpls.2021.634397
- [7] O’Sullivan CA, Belt K, Thatcher LF. Tackling control of a cosmopolitan phytopathogen: sclerotinia. *Front Plant Sci*. 2021;12:707509. doi: 10.3389/fpls.2021.707509
- [8] Xin XF, Kvitko B, He S. *Pseudomonas syringae*: what it takes to be a pathogen. *Nat Rev Microbiol*. 2018;16:316–328. doi: 10.1038/nrmicro.2018.17
- [9] Dhaouadi S, Mougou AH, Rhouma A. The plant pathogen *Rhodococcus fascians*. History, disease symptomatology, host range, pathogenesis and plant–pathogen interaction. *Ann Appl Biol*. 2020;177:4–15. doi: 10.1111/aab.12600
- [10] European Commission: Opinion on azole antimycotic resistance. https://food.ec.europa.eu/system/files/2020-12/sci-com_ssc_out278_en.pdf
- [11] Smith K, Evans DA, El-Hiti GA. Role of modern chemistry in sustainable arable crop protection. *Phil Trans R Soc B*. 2008;363:623–637. doi: 10.1098/rstb.2007.2174
- [12] Hellin P, King R, Urban M, et al. The adaptation of *fusarium culmorum* to DMI fungicides is mediated by major transcriptome modifications in response to azole fungicide, including the overexpression of a PDR transporter (FcABC1). *Front Microbiol*. 2018;9:1385. doi: 10.3389/fmicb.2018.01385
- [13] Berger S, Chazli YE, Babu AF, et al. Azole resistance in *Aspergillus fumigatus*: a consequence of antifungal use in agriculture? *Front Microbiol*. 2017;8:1024. doi: 10.3389/fmicb.2017.01024
- [14] Damalas CA, Eleftherohorinos IG. Pesticide exposure, safety issues, and risk assessment indicators. *Int J Environ Res Public Health*. 2011;8(5):1402–1419. doi: 10.3390/ijerph8051402
- [15] Pacholak A, Burlaga N, Frankowski R, et al. Azole fungicides: (Bio)degradation, transformation products and toxicity elucidation. *Sci Total Environ*. 2022;802:149917. doi: 10.1016/j.scitotenv.2021.149917
- [16] O’Kennedy R, Thornes RD. Coumarins: biology, applications and mode of action. New York: Wiley Chichester; 1997.
- [17] Matos MJ, Santana L, Uriarte E, et al. Coumarins — an important class of phytochemicals. In: *Phytochemicals - isolation, characterisation and role in human health*. InTech; 2015. doi: 10.5772/59982
- [18] Annunziata F, Pinna C, Dallavalle S, et al. An overview of coumarin as a versatile and readily accessible scaffold with broad-ranging biological activities. *Int J Mol Sci*. 2020;21(13):4618. doi: 10.3390/ijms21134618
- [19] Song PP, Zhao J, Liu Z-L, et al. Evaluation of antifungal activities and structure–activity relationships of coumarin derivatives. *Pest Manag Sci*. 2017;73:94–101. doi: 10.1002/ps.4422
- [20] Wei Y, Peng W, Wanf D, et al. Design, synthesis, antifungal activity, and 3D-QSAR of coumarin derivatives. *J Pestic Sci*. 2018;43:88–95. doi: 10.1584/jpestics.D17-075
- [21] Guo Y, Chen J, Ren D, et al. Synthesis of osthol-based botanical fungicides and their antifungal application in crop protection. *Bioorg Med Chem*. 2021;40:116184. doi: 10.1016/j.bmc.2021.116184
- [22] Xin W, Mao Y, Lu F, et al. In vitro fungicidal activity and in planta control efficacy of coumoxystrobin against *Magnaporthe oryzae*. *Pestic Biochem Phys*. 2020;162:78–85. doi: 10.1016/j.pestbp.2019.09.004
- [23] Zhang S-G, Wan Y-Q, Wen Y, et al. Novel coumarin 7-carboxamide/sulfonamide derivatives as potential fungicidal agents: design, synthesis, and biological evaluation. *Molecules*. 2022;27(20):6904. doi: 10.3390/molecules27206904
- [24] Chen J, Yu Y, Li S, et al. Resveratrol and coumarin: novel agricultural antibacterial agent against *Ralstonia solanacearum* in vitro and in vivo. *Molecules*. 2016;21:1501. doi: 10.3390/molecules21111501
- [25] Dekić BD, Radulović NS, Dekić VS, et al. Synthesis and antimicrobial activity of new 4-heteroaryl amino coumarin derivatives containing nitrogen and sulfur as heteroatoms. *Molecules*. 2010;15:2246–2256. doi: 10.3390/molecules15042246

- [26] Rastija V, Vrandečić K, Ćosić J, et al. Biological activities related to plant protection and environmental effects of coumarin derivatives: QSAR and molecular docking studies. *Int J Mol Sci.* 2021;22(14):7283. doi: [10.3390/ijms22147283](https://doi.org/10.3390/ijms22147283)
- [27] Pavela R, Maggi F, Benelli G. Coumarin (2H-1-benzopyran-2-one): a novel and eco-friendly aphicide. *Nat Prod Res.* 2021;35(9):1566–1571. doi: [10.1080/14786419.2019.1660334](https://doi.org/10.1080/14786419.2019.1660334)
- [28] Zhang TJ, Ma Z, Ma H, et al. Metabolic pathways modulated by coumarin to inhibit seed germination and early seedling growth in *Eleusine indica*. *Plant Physiol Biochem PPB.* 2023;203:108035. doi: [10.1016/j.plaphy.2023.108035](https://doi.org/10.1016/j.plaphy.2023.108035)
- [29] Gao H, Shreeve JNM. Azole-based energetic salts. *Chem Rev.* 2011;111:7377–7436. doi: [10.1021/cr200039c](https://doi.org/10.1021/cr200039c)
- [30] Küçükgülmez ŞG, Çıkla-Süzcü P. Recent advances bioactive 1,2,4-triazole-3-thiones. *Eur J Med Chem.* 2015;97:830–870. doi: [10.1016/j.ejmech.2014.11.033](https://doi.org/10.1016/j.ejmech.2014.11.033)
- [31] Aggarwal R, Sumran G. An insight on medicinal attributes of 1,2,4-triazoles. *Eur J Med Chem.* 2020;205:112652. doi: [10.1016/j.ejmech.2020.112652](https://doi.org/10.1016/j.ejmech.2020.112652)
- [32] Tang R, Jin L, Mou C, et al. Synthesis, antifungal and antibacterial activity for novel amide derivatives containing a triazole moiety. *Chem Cent J.* 2013;7:30. doi: [10.1186/1752-153X-7-30](https://doi.org/10.1186/1752-153X-7-30)
- [33] Shao WB, Wang PY, Fang ZM, et al. Synthesis and biological evaluation of 1,2,4-triazole thioethers as both potential virulence factor inhibitors against plant bacterial diseases and agricultural antiviral agents against tobacco mosaic virus infections. *J Agric Food Chem.* 2021;69(50):15108–15122. doi: [10.1021/acs.jafc.1c05202](https://doi.org/10.1021/acs.jafc.1c05202)
- [34] Keshavarz H, Khodabin G. The role of uniconazole in improving physiological and biochemical attributes of bean (*Phaseolus vulgaris* L.) subjected to drought stress. *J Crop Sci Biotechnol.* 2019;22:161–168. doi: [10.1007/s12892-019-0050-0](https://doi.org/10.1007/s12892-019-0050-0)
- [35] Fletcher RA, Gilley A, Davis TD, et al. Triazoles as plant growth regulators and stress protectants. *Hortic Rev.* 2000;24:55–138. doi: [10.1002/9780470650776.ch3](https://doi.org/10.1002/9780470650776.ch3)
- [36] Hajhashemi S. Physiological, biochemical, antioxidant and growth characterizations of gibberellin and paclobutrazol-treated sweet leaf (*Stevia rebaudiana* B.) herb. *J Plant Biochem Biotechnol.* 2017;27(2):237–240. doi: [10.1007/s13562-017-0428-4](https://doi.org/10.1007/s13562-017-0428-4)
- [37] Buchenauer H. Mechanism of action of triazolyl fungicides and related compounds. In: Lyr H, Buchenauer H, editor. *Modern selective fungicides: properties, applications, mechanisms of action.* Harlow: Longman Scientific and Technical; 1987. p. 205–231.
- [38] Monk BC, Sagatova AA, Hosseini P, et al. Fungal Lanosterol 14 α -demethylase: a target for next-generation antifungal design. *Biochim Biophys Acta Proteins Proteom.* 2020;1868(3):140206. doi: [10.1016/j.bbapap.2019.02.008](https://doi.org/10.1016/j.bbapap.2019.02.008)
- [39] Karlaš M, Rastija V, Šubarić D, et al. Green synthesis and acetylcholinesterase inhibition of coumarin-1,2,4-triazole hybrids. *Curr Org Chem.* 2023;27:883–892. doi: [10.2174/1385272827666230817145725](https://doi.org/10.2174/1385272827666230817145725)
- [40] Jayashree BS, Sahu AR, Srinivasa MM, et al. Synthesis, characterization and determination of partition coefficient of some triazole derivatives of coumarins for their anti-microbial activity. *Asian J Chem.* 2007;19:73–78.
- [41] Kokil GR, Rewatkar PV, Gosain S, et al. Synthesis and in vitro evaluation of novel 1, 2, 4-triazole derivatives as antifungal agents. *Lett Drug Des Discov.* 2010;7:46–49. doi: [10.2174/157018010789869415](https://doi.org/10.2174/157018010789869415)
- [42] Shi Y, Zhou CH. Synthesis and evaluation of a class of new coumarin triazole derivatives as potential antimicrobial agents. *Bioorg Med Chem Lett.* 2011;21(3):956–960. doi: [10.1016/j.bmcl.2010.12.059](https://doi.org/10.1016/j.bmcl.2010.12.059)
- [43] Panda SS, Malik R, Chand M, et al. Synthesis and antimicrobial activity of some new 4-triazolylmethoxy-2H-chromen-2-one derivatives. *Med Chem Res.* 2012;21:3750–3756. doi: [10.1007/s00044-011-9881-0](https://doi.org/10.1007/s00044-011-9881-0)
- [44] Damu GL, Cui SF, Peng XM, et al. Synthesis and bioactive evaluation of a novel series of coumarinazoles. *Bioorg Med Chem Lett.* 2014;24(15):3605–3608. doi: [10.1016/j.bmcl.2014.05.029](https://doi.org/10.1016/j.bmcl.2014.05.029)
- [45] Molnar M, Periš I, Komar M. Choline chloride based deep eutectic solvents as a tuneable medium for synthesis of Coumarinyl 1,2,4-triazoles: effect of solvent type and temperature. *Eur J Org Chem.* 2019;15:2688–2694. doi: [10.1002/ejoc.201900249](https://doi.org/10.1002/ejoc.201900249)
- [46] Reddy KR, Mamatha R, Babu MSS, et al. Synthesis and antimicrobial activities of some triazole, thiadiazole, and oxadiazole substituted coumarins. *J Heterocycl Chem.* 2014;51(1):132–137. doi: [10.1002/jhet.1745](https://doi.org/10.1002/jhet.1745)
- [47] Al-Amiery AA, Musa AY, Kadhum AA, et al. The use of umbelliferone in the synthesis of new heterocyclic compounds. *Molecules.* 2011;16(8):6833–6843. doi: [10.3390/molecules16086833](https://doi.org/10.3390/molecules16086833)
- [48] Siber T, Bušić V, Zobundžija D, et al. An improved method for the quaternization of nicotinamide and antifungal activities of its derivatives. *Molecules.* 2019;24:1001. doi: [10.3390/molecules24061001](https://doi.org/10.3390/molecules24061001)
- [49] Bušić V, Vrandečić K, Siber T, et al. A rapid microwave induced synthesis of isonicotinamide derivatives and their antifungal activity. *Croat Chem Acta.* 2019;92:125–135. doi: [10.5562/cca3527](https://doi.org/10.5562/cca3527)
- [50] Statistica 14.1.0. TIBCO, Santa Clara, CA, USA; 2023.
- [51] Wiegand I, Hilpert K, Hanckok REW. Agar and broth dilution methods to determine the minimal inhibitory concentration (MIC) of antimicrobial substances. *Nat Protoc.* 2008;3:163–175. doi: [10.1038/nprot.2007.521](https://doi.org/10.1038/nprot.2007.521)
- [52] Hanwell MD, Curtis DE, Lonie DC, et al. Avogadro: an advanced semantic chemical editor, visualization, and analysis platform. *J Cheminform.* 2012;4(1):17. doi: [10.1186/1758-2946-4-17](https://doi.org/10.1186/1758-2946-4-17)
- [53] Hocquet A, Langgård M. An evaluation of the MM+ force field. *J Mol Model.* 1998;4:94–112. doi: [10.1007/s008940050128](https://doi.org/10.1007/s008940050128)
- [54] Stewart JJP. Optimization of parameters for semiempirical methods I. Method. *J Comput Chem.* 1989;10:209–220. doi: [10.1002/jcc.540100208](https://doi.org/10.1002/jcc.540100208)
- [55] Tetko IV, Gasteiger J, Todeschini R, et al. Virtual computational chemistry laboratory – design and description. *J Comput Aided Mol Des.* 2005;19:453–463. doi: [10.1007/s10822-005-8694-y](https://doi.org/10.1007/s10822-005-8694-y)
- [56] Gramatica P, Chirico N, Papa E, et al. QSARINS: a new software for the development, analysis, and validation of QSAR MLR models. *J Comput Chem.* 2013;34:2121–2132. doi: [10.1002/jcc.23361](https://doi.org/10.1002/jcc.23361)
- [57] Gramatica P. Principles of QSAR modeling: comments and suggestions from personal experience. *IJQSPR.* 2020;5:61–97. doi: [10.4018/IJQSPR.20200701.0a1](https://doi.org/10.4018/IJQSPR.20200701.0a1)
- [58] Tropsha A, Gramatica P, Gombar VK. The importance of being earnest: validation is the absolute essential for successful application and interpretation of QSPR models. *QSAR Comb Sci.* 2003;22:69–77. doi: [10.1002/qsar.200390007](https://doi.org/10.1002/qsar.200390007)
- [59] Gramatica P. Principles of QSAR models validation: internal and external. *QSAR Comb Sci.* 2007;26:694–701. doi: [10.1002/qsar.200610151](https://doi.org/10.1002/qsar.200610151)

- [60] Consonni V, Ballabio D, Todeschini R. Comments on the definition of the Q2 parameter for QSAR validation. *J Chem Inf Model.* 2009;49(7):1669–1678. doi: [10.1021/ci900115y](https://doi.org/10.1021/ci900115y)
- [61] Eriksson L, Jaworska J, Worth AP, et al. Methods for reliability and uncertainty assessment and for applicability evaluations of classification- and regression-based QSARs. *Environ Health Perspect.* 2003;111(10):1361–1375. doi: [10.1289/ehp.5758](https://doi.org/10.1289/ehp.5758)
- [62] Trott O, Olson AJ. AutoDock Vina: improving the speed and accuracy of docking with a new scoring function, efficient optimization, and multithreading. *J Comput Chem.* 2010;31(2):455–461. doi: [10.1002/jcc.21334](https://doi.org/10.1002/jcc.21334)
- [63] Tyndall JD, Sabherwal M, Sagatova AA, et al. Structural and functional elucidation of yeast lanosterol 14 α -demethylase in complex with agrochemical antifungals. *PLoS One.* 2016;11(12):e0167485. doi: [10.1371/journal.pone.0167485](https://doi.org/10.1371/journal.pone.0167485)
- [64] Morris GM, Huey R, Lindstrom W, et al. AutoDock4 and AutoDockTools4: automated docking with selective receptor flexibility. *J Comput Chem.* 2009;30(16):2785–2791. doi: [10.1002/jcc.21256](https://doi.org/10.1002/jcc.21256)
- [65] Dassault Systemes BIOVIA Discovery studio visualizer, release 2016. Dassault Systemes Biovia Corp, San Diego, CA, USA; 2017.
- [66] Herkert PF, Al-Hatmi AMS, de Oliveira Salvador GL, et al. Molecular characterization and antifungal susceptibility of clinical fusarium species from Brazil. *Front Microbiol.* 2019;10:737. doi: [10.3389/fmicb.2019.00737](https://doi.org/10.3389/fmicb.2019.00737)
- [67] Yi Y, de Jong A, Frenzel E, et al. Comparative transcriptomics of *bacillus mycooides* strains in response to potato-root exudates reveals different genetic adaptation of endophytic and soil isolates. *Front Microbiol.* 2017;8:1487. doi: [10.3389/fmicb.2017.01487](https://doi.org/10.3389/fmicb.2017.01487)
- [68] Griebisch A, Matschiavelli N, Lewandowska S, et al. Presence of *bradyrhizobium* sp. under continental conditions in central Europe. *Agriculture.* 2020;10(10):446. doi: [10.3390/agriculture10100446](https://doi.org/10.3390/agriculture10100446)
- [69] Kiralj R, Ferreira MMC. Basic validation procedures for regression models in QSAR and QSPR studies: theory and application. *J Braz Chem Soc.* 2009;20(4):770–787. doi: [10.1590/S0103-50532009000400021](https://doi.org/10.1590/S0103-50532009000400021)
- [70] Masand VH, Mahajan DT, Nazeruddin GM, et al. Effect of information leakage and method of splitting (rational and random) on external predictive ability and behavior of different statistical parameters of QSAR model. *Med Chem Res.* 2015;24:1241–1264. doi: [10.1007/s00044-014-1193-8](https://doi.org/10.1007/s00044-014-1193-8)
- [71] Todeschini R, Consonni V. *Molecular descriptors for chemoinformatics.* Chichester: Wiley-VCH; 2009.
- [72] Consonni V, Todeschini R, Pavan M. Structure/response correlations and similarity/diversity analysis by GET-AWAY descriptors. 1. Theory of the novel 3D molecular descriptors. *J Chem Inf Comput Sci.* 2002;42(3):682–692. doi: [10.1021/ci015504a](https://doi.org/10.1021/ci015504a)
- [73] Devinyak O, Havrylyuk D, Lesyk R. 3D-MoRSE descriptors explained. *J Mol Graph Model.* 2014;54:194–203. doi: [10.1016/j.jmglm.2014.10.006](https://doi.org/10.1016/j.jmglm.2014.10.006)
- [74] Zhang J, Li L, Lv Q, et al. The fungal CYP51s: their functions, structures, related drug resistance, and inhibitors. *Front Microbiol.* 2019;10:691. doi: [10.3389/fmicb.2019.00691](https://doi.org/10.3389/fmicb.2019.00691)
- [75] Wang R, Lu Y, Wang S. Comparative evaluation of 11 scoring functions for molecular docking. *J Med Chem.* 2003;46(12):2287–2303. doi: [10.1021/jm0203783](https://doi.org/10.1021/jm0203783)
- [76] Brenk R, Vetter SW, Boyce SE, et al. Probing molecular docking in a charged model binding site. *J Mol Biol.* 2006;357(5):1449–1470. doi: [10.1016/j.jmb.2006.01.034](https://doi.org/10.1016/j.jmb.2006.01.034)